Materials Letters 122 (2014) 216–219

Contents lists available at ScienceDirect

Materials Letters

journal homepage: www.elsevier.com/locate/matlet

Ethylenediamine (EDA) – assisted hydrothermal synthesis of nitrogen-doped Bi_2WO_6 powders

Gangqiang Zhu [a,*], Jia Liang [a], Mirabbos Hojamberdiev [b], Sara Aldabe Bilmes [c], Xiumei Wei [a], Peng Liu [a], Jianping Zhou [a]

[a] School of Physics and Information Technology, Shaanxi Normal University, Xi'an 710062, PR China
[b] Materials and Structures Laboratory, Tokyo Institute of Technology, 4259 Nagatsuta, Midori, Yokohama, Kanagawa 226-8503, Japan
[c] Instituto de Química Física de los Materiales, Medio Ambiente y Energía (INQUIMAE), Facultad de Ciencias Exactas y Naturales, Universidad de Buenos Aires, Pabellón II, Ciudad Universitaria, C1428EHA Buenos Aires, Argentina

ARTICLE INFO

Article history:
Received 5 January 2014
Accepted 13 February 2014
Available online 19 February 2014

Keywords:
Semiconductors
Nitrogen doping
Hydrothermal synthesis
Nanocrystalline materials
Photocatalytic activity
Visible light irradiation

ABSTRACT

Novel nitrogen-doped Bi_2WO_6 (N-BWO) powders were synthesized by an ethylenediamine-assisted hydrothermal method. The obtained results indicated that the N-BWO powders are composed of microstructures self-assembled from single-crystalline nanosheets. The doped nitrogen was substituted for oxygen in the crystal lattice of Bi_2WO_6, causing a red shift (from 2.82 to 2.63 eV) for N-BWO powders compared to pure BWO. The as-synthesized N-BWO powders exhibited an efficient visible light-induced photocatalytic activity toward the degradation of Rhodamine B (RhB) in aqueous solution due to their enhanced visible light absorption and special layered microstructures.

1. Introduction

Bi_2WO_6 (BWO), one of the simplest members of the Aurivillius oxide family, has attracted significant attention due to its unique physical and chemical properties [1]. Recent studies have demonstrated that BWO also possesses a visible light-induced photocatalytic activity for degradation of organic contaminants [2]. However, the photocatalytic activity of BWO is low due to the fast recombination of photogenerated electron–hole pairs [3]. Therefore, it is necessary to suppress the recombination of electrons and holes. In recent years, the modifications of BWO with semiconductor [4] and doped with ions [3,5,6] have been demonstrated to inhibit the recombination of electron–hole pairs successfully.

It is well-known that nano-sized photocatalysts usually have a high photocatalytic activity because of their special morphologies, large specific surface areas, and high efficiency of electron–hole separation. Therefore, considerable efforts have been made to the fabrication of nano-sized BWO to improve its photocatalytic performance, and a wide variety of BWO nanostructures, such as nanoparticles, nanoplates, hollow nanostructures and 3D hierarchical nanostructures, have been fabricated by various methods in recent years [7–10]. Nevertheless, the controlled self-assembly of nanostructures into desired architectures via a facile and effective approach still remains challenging.

In this work, the N-BWO powders, composed of single-crystalline nanosheets, with high specific surface area were synthesized by an ethylenediamine-assisted hydrothermal method, and their visible light-induced photocatalytic activity was evaluated for the degradation of RhB in aqueous solution in comparison to that of pure BWO.

2. Experimental

Synthesis: All chemical with analytical purity were obtained from Shanghai Chemical Reagent Factory of China and were used without further purification. In a typical synthesis procedure of N-BWO, 2 mmol of $Bi(NO_3)_3 \cdot 5\,H_2O$ was dissolved in 20 mL of 1 M HNO_3 to form a clear solution, and 1 mmol of Na_2WO_4 was dissolved in 50 mL of deionized water. Afterward, both solutions were mixed together under magnetic stirring, and a white precipitate was formed quickly. The pH of the suspension was adjusted to 6 by adding ethylenediamine. After a constant stirring for 20 min, the well-homogenized mixture was transferred into a 100 mL Teflon-lined stainless steel autoclave and filled with deionized water up to 80% of the total volume. The autoclave was sealed, maintained at 180 °C for 16 h, and cooled down to

* Corresponding author. Tel./fax: +86 29 81530750.
E-mail address: zgq2006@snnu.edu.cn (G. Zhu).

http://dx.doi.org/10.1016/j.matlet.2014.02.044
0167-577X

room temperature naturally. The resulting precipitate was then collected, washed with deionized water and dried at 80 °C. The pure BWO nanostructures were performed via the same hydrothermal synthesis process just using 0.1 mol/L NaOH aqueous solution to adjust the pH to 6.

Characterization: The X-ray diffraction (XRD) patterns were recorded on a D/Max2550 X-ray diffractometer with Cu Kα radiation. The morphologies of the samples were examined using an S-4800 scanning electron microscope. The transmission electron microscopic (TEM) and high-resolution transmission electron microscopic (HRTEM) images and selected area electron diffraction (SAD) pattern of the samples were taken with a JEM-2100 electron microscope (JEOL, Japan). The crystalline phases were also confirmed by a T64000 Raman spectrometer (Horiba Jobin Yvon S.A.S., France) with an Ar laser (514.5 nm). X-ray photoelectron spectroscopy (XPS) analysis was performed on an ESCALAB MKII X-ray photoelectron spectrometer (VG Scientific, UK) using Mg Kα radiation. The UV–vis absorbance spectra of the samples were obtained using a Lambda 950 UV–vis–NIR spectrophotometer. The specific surface area (S_{BET}) and pore size distribution (PSD) were obtained from N_2 adsorption–desorption isotherms at 77 K (ASAP 2010, Micromeritics, USA), on samples preheated at 120 °C for 12 h in vacuum.

Photodegradation experiments: As a kind of poisonous synthetic dyes, RhB is widely used in various industrial fields. The photocatalytic degradation of Rhodamine B (RhB) in aqueous solution was performed under visible light using 300 W Xe lamps with a 420 nm cut-off filter. The initial concentration of RhB was 10 mg/L, and the catalyst was 1.0 g/L. The suspensions were first sonicated for 10 min and then stirred in the dark for 30 min to ensure adsorption–desorption equilibrium prior to visible light irradiation. During the photodegradation process, 2 mL of the suspension was taken out at a given time interval for s subsequent analysis of RhB concentration. The RhB concentration was analyzed by U-3010 UV–vis spectrophotometer (Hitachi, Japan).

3. Results and discussion

Fig. 1a shows the XRD patterns of pure BWO and N-BWO powders. All the XRD peaks can be indexed to the orthorhombic BWO (JCPDS card no. 73-1126). According to the intensity of the XRD peaks, it can be said that pure BWO and N-BWO powders are well-crystallized. To confirm successful nitrogen doping in BWO, the prepared samples were analyzed by Raman and X-ray photoelectron spectroscopy.

In the Raman spectrum of pure BWO in Fig. 1b, the bands at 793 and 850 cm^{-1} are attributed to the asymmetric and symmetric A_g modes of terminal O–W–O, and the band at 723 cm^{-1} is associated with the tungstate chain. The band at 306 cm^{-1} is related to the translational mode involving simultaneous motions of Bi^{3+} and WO^{6-} [11]. When N atoms were doped into BWO, the intensity of the bands changed. The intensity of the band at 850 cm^{-1} decreased, whereas the bands at 850, 793, and 723 cm^{-1} shifted towards lower frequencies. These changes might be related to nitrogen doping into the O–W–O lattice, and the doped nitrogen atoms replaced some oxygen atoms that were originally bonded with W. The results of Raman spectroscopy analysis confirm that N atoms were inserted into the crystal lattice of BWO. The wide XPS survey spectra of pure BWO and N-BWO powders are shown in Fig. 1c, in which the N 2p peak at 400 eV can be observed for the N-BWO powders compared with pure BWO. The enlarged N 2p peak is comparatively shown in Fig. 1d which proves N doping in the BWO powders.

The SEM micrographs of the samples are shown in Fig. 2. As shown in Fig. 2a, pure BWO powders have flower-like structures assembled from lots of nanosheets with the thickness of

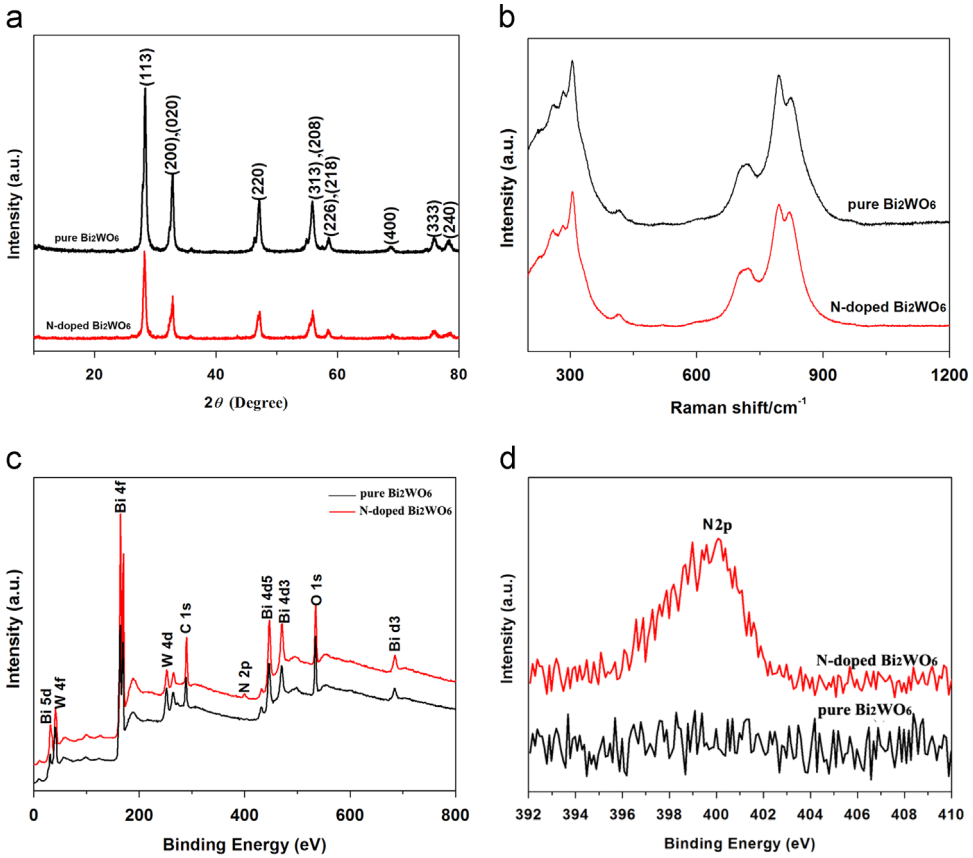

Fig. 1. XRD patterns (a), Raman spectra (b), and XPS spectra (c and d) of pure BWO and N-BWO powders.

20 nm. Fig. 2b shows the SEM micrograph of pure BWO powders synthesized with EDA. However, N-BWO powders prepared with EDA have plate-like structures along with nanostructures. Fig. 2c shows a magnified SEM micrograph of N-BWO powders, confirming the formation of microstructures from self-assembly of nanosheets with the thickness of 20 nm. As can be seen in the SEM micrographs shown in Fig. 2d–f, the N-BWO powders have also some flower-like microstructures composed of nanosheets. The above-demonstrated results indicate that the EDA greatly affected the overall morphology of the final N-BWO products. The formation mechanisms are currently being investigated and will be presented in our forthcoming report.

Fig. 3a shows a typical TEM image of the N-doped Bi_2WO_6 nanostructures, which confirms that the N-BWO structures are composed of nanosheets. The HRTEM image shown in Fig. 3b indicates that the N-BWO nanosheets are single-crystal structures, and the two lattice fringes of 0.27 nm in the observed crystallite agree well with the (200) and (020) lattice planes of BWO. The SAD pattern, shown as an inset in Fig. 3b, also confirms that the N-BWO nanosheets were formed as single-crystal structures.

Fig. 4 shows the UV–vis absorbance spectra of pure BWO and N-BWO powders. Comparing to pure BWO, a red-shift was observed for the N-BWO powders. The optical data of pure BWO and N-BWO powders were analyzed at near absorption edge using the equation: $\alpha h\nu = A(h\nu - E_g)^{n/2}$. On the basis of the results obtained from the equation, a plot of $(\alpha h\nu)^2$ versus $h\nu$ is shown as an inset in Fig. 4. The calculated optical band gaps of pure BWO and N-BWO powders are 2.82 and 2.63 eV, respectively. The obtained results suggest that the N-BWO powders are more effective in absorbing visible light, which will enhance photocatalytic activity under visible light.

Fig. 4b shows the N_2 adsorption–desorption isotherms of pure BWO and N-BWO powders. As shown in Fig. 4b, these isotherms can be categorized as type II, according to IUPAC classification, with a significant hysteresis loop observed, which implies the presence of mesopores (2–70 nm in size). These results are further confirmed by the corresponding pore-size distribution curves (inset in Fig. 4b), in which the peaks for both mesopores and macropores can be found. The smaller pores might be generated during the crystal growth process, whereas the larger pores can be attributed to the voids between the intercrossed BWO nanosheets. The S_{BET} values of pure BWO and N-BWO powders calculated from N_2 adsorption isotherms are 23.1 and 28.6 m^2/g, respectively.

Fig. 4c shows the variation of RhB concentration (C/C_0) in aqueous solution over pure BWO and N-BWO powders under visible light irradiation. It is noted that the N-BWO powders exhibited higher photocatalytic activity than pure BWO powders for the photodegradation of RhB under visible light. The total photodegradation of RhB with N-BWO powders was 99.3% within

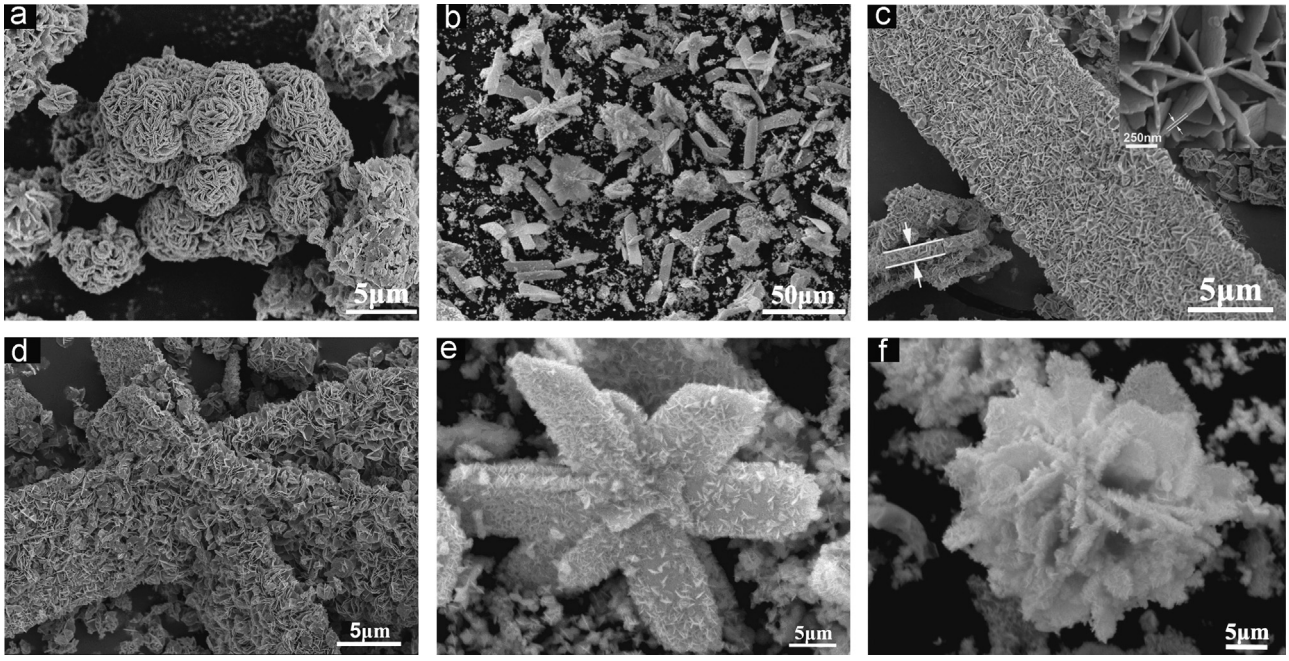

Fig. 2. SEM micrographs of pure BWO (a and b) and N-BWO (c–f) powders.

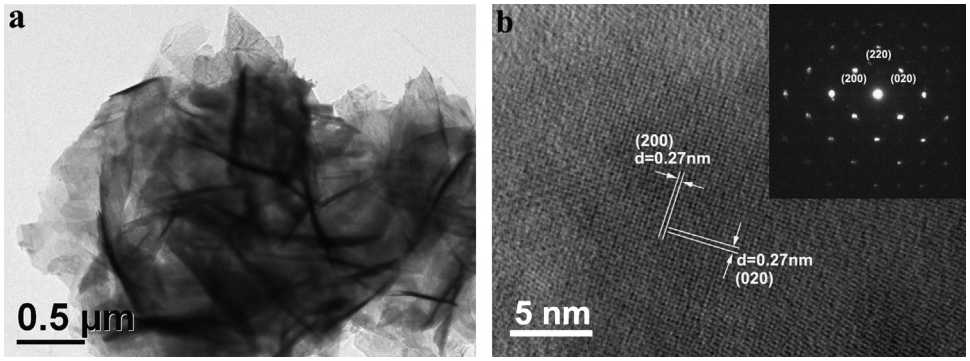

Fig. 3. TEM (a) and HRTEM (b) images and SAD pattern (inset) of N-BWO powders.

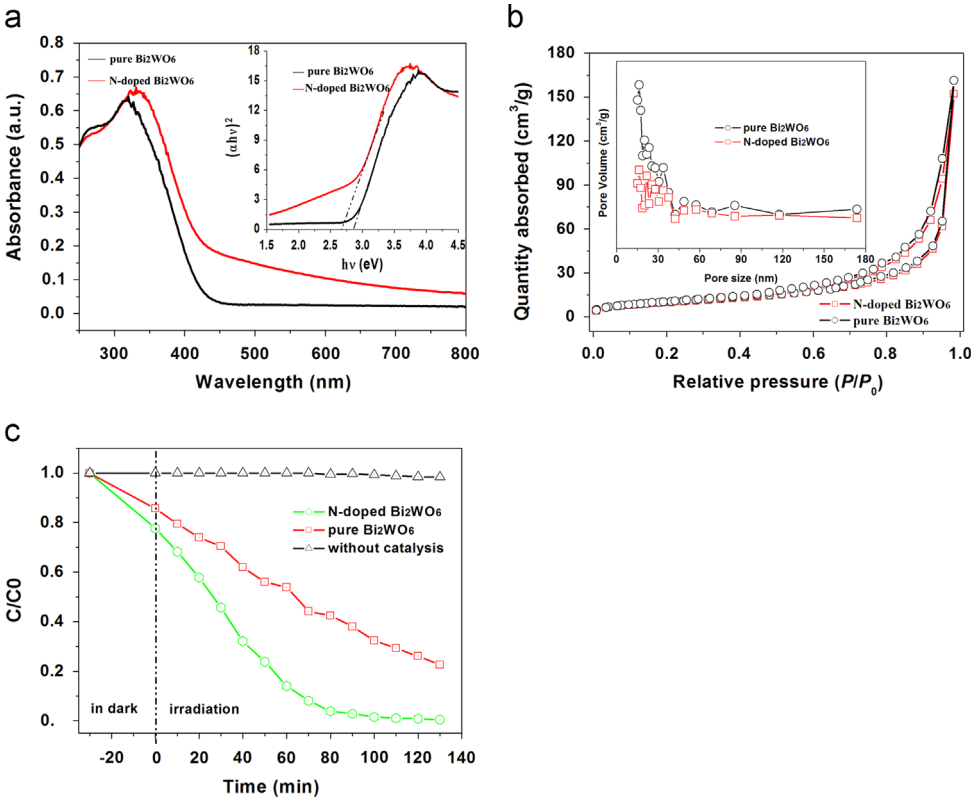

Fig. 4. UV–vis spectra (a), N_2 adsorption–desorption isotherms (b), and photocatalytic activity (c) of pure BWO and N-BWO powders.

100 min of visible light irradiation while the total photodegradation of RhB with pure BWO powders was 67.0%. It is clear that the N-BWO powders showed an improved visible-light-induced photocatalytic activity for the degradation of RhB in aqueous solution due to enhanced visible light absorption and special layered microstructures. Nitrogen doping has often been employed to increase visible light absorption by elevating the valence band maximum to narrow the band-gap with N 2p states or forming some localized N 2p states in the band-gap [12].

4. Conclusions

In summary, an ethylenediamine-assisted hydrothermal method was developed for the synthesis of novel N-BWO powders. The N-BWO microstructures composed of nanosheets showed an improved photocatalytic activity for the degradation of RhB under visible light due to enhanced visible light absorption and special layered microstructures. The N-BWO microstructures obtained can be considered as a good candidate for visible-light-responsive photocatalyst.

Acknowledgments

This work was supported by the National Natural Science Foundation of China (Program nos. 51102160 and 11104175) and Innovation Funds of Graduate Programs, SNNU. (Program no. 2013CXS011). MH would like to thank the Japan Society for the Promotion of Science (JSPS) for financial support.

References

[1] Kim N, Vannier R-N, Grey CP. Chem Mater 2005;17:1952–8.
[2] Tang J, Zou Z, Ye J. Catal Lett 2004;92:53–6.
[3] Huang Y, Ai Z, Ho W, Chen M, Lee SJ. Phys Chem C 2010;114:6342–9.
[4] Zhang L, Wong K-H, Chen Z, Yu JC, Zhao J, Hu C, et al. Appl Catal A 2009;363:221–9.
[5] Shang M, Wang W, Zhang L, Xu H. Mater Chem Phys 2010;120:155–9.
[6] Sun Z, Li X, Guo S, Wang H, Wu ZJ. Colloid Interface Sci 2013;412:31–8.
[7] Mann AKP, Skrabalak SE. Chem Mater 2011;23:1017–22.
[8] Liu Y, Li Z, Lv H, Tang H, Xing X. Mater Lett 2013;108:84–7.
[9] Hu S-P, Xu C-Y, Zhen L. Mater Lett 2013;95:117–20.
[10] Chen Z, Qian L, Zhu J, Yuan Y, Qian X. CrystEngComm 2010;12:2100–6.
[11] Zhang L-W, Wang Y-J, Cheng H-Y, Yao W-Q, Zhu Y-F. Adv Mater 2009;21:1286–90.
[12] Ullah R, Sun H, Ang HM, Tadé MO, Wang S. Ind Eng Chem Res 2013;52:3320–8.